

# Shear Strength of Cross Laminated Timber Based on Larch Lamina Combination

Seung-Youp Baek, Yo-Jin Song, and Soon-Il Hong \*

Cross-laminated timber (CLT) fails in the outermost tensile lamina under bending loads, or rolling shear failure occurs in the Minoir direction lamina. This study investigated the effect of lamina width (90 mm, 120 mm), modulus of elasticity (MOE), and placement of major direction lamina on the shear strength of *Larix kaempferi* Carr CLT. The shear test was conducted using the short span bending test. Results showed that the specimen with 90 mm width of lamina underwent rolling shear failure at the minor direction lamina. The specimen with 120 mm width of lamina had suppressed rolling shear failure and failed at the outermost tensile lamina, which resulted in 52% higher shear strength compared to the 90 mm width specimen. CLT with high MOE placed in the outermost tensile lamina had increased shear strength. The specimen with four laminas in the major direction had both the highest strength and the lowest reliability due to the high standard deviation. This suggested that the width of the larch lamina and the MOE affect the strength of CLT. The CLT strength obtained using the FEA and the theoretical analysis were compared with the measured strength values.

DOI: 10.15376/biores.19.3.4366-4380

Keywords: *Larix kaempferi* Carr; Cross laminated timber; FEM; Shear strength

Contact information: Department of Forest Biomaterials Engineering, Kangwon National University, 1- Kangwondaehak-gil, ChunCheon-si, Gangwon-do, 24341, Republic of Korea;

\* Corresponding author: hongsi@kangwon.ac.kr

## INTRODUCTION

Cross-laminated timber (CLT) is a structural wood panel manufactured with at least three odd laminas by bonding laminas using adhesives (mechanical connections, such as self-tapping screws) after placement of the adjacent laminas so that the grain direction is orthogonal to each other (Schmidt and Griffin, 2009). When CLT is used as a flooring material, shear deformation is caused by the relatively low rolling shear stiffness of the orthogonally laminated minor direction lamina, which results in rolling shear failure of the minor direction lamina even under low load capacity. This rolling shear is an important design factor for out-of-plane loading of CLT under short-span bending loads and centralized loads (Rahman *et al.* 2020). In CLT flooring design, shear strength is used as the rolling shear strength of CLT panels (CSA 086, 2018). The lamina comprising the CLT can affect the shear strength of the CLT (Wang *et al.* 2018; Ehrhart and Brandner 2018). Navaratnam *et al.* (2020) found that the elastic modulus of lamina significantly affected the shear strength of CLT in Australian Radiata pine tree species. Li *et al.* (2021) confirmed that the shear strength value of CLT increases as the height-thickness ratio of the lamina increases. Furthermore, Zhou *et al.* (2014) mentioned that when the width of the lamina is the same, the shear load-bearing capacity of CLT decreases when thickness increases. Consequently, the CLT handbook (2011) and KS F 2081(2021) standards specify the width

of the lamina as 2.5 times the thickness, while a width that is 3.5 times the thickness is recommended in Canadian Standards Association (CSA). Since the lamina comprising CLT is milled from medium diameter wood, lamina sizes ranging from 10 to 50 mm thick and 60 to 180 mm wide are used, while spruce-pine-fir (SPF) species use lamina sizes ranging from 38 mm thick and 89 mm wide to 140 mm wide (Zhou *et al.* 2014).

In domestic wood construction, domestic *Larix kaempferi* Carr., which accounts for 73% of the general sawmilling industry, is mainly used because of its higher specific gravity compared to other coniferous woods, as well as its excellent mechanical properties, making it suitable for use as a structural material (Lee *et al.* 2018). Domestic *Larix kaempferi* Carr. is mainly used in medium-sized lumber with an average diameter of 240 mm (Chong *et al.* 2014), and lamina that are 30 mm thick and 90 mm and 120 mm wide are primarily used (Kwon *et al.* 2013). However, there is a lack of research on the shear strength of CLT as a function of lamina width. Therefore, this study investigated how larch lamina widths of 90 and 120 mm, the elastic modulus of the lamina, and the placement of major and minor direction lamina affect the shear strength of CLT.

There are two methods of testing the shear strength of CLT: planer shear test and short span bending test. In the planer shear test, a small specimen is fabricated, and compressive shear is applied to both end faces of the specimen (EN 16351, 2015). In the short span bending test, large shear loads are applied by reducing the span to depth ratio, resulting in rolling shear failure in the minor direction lamina of CLT (ASTM D198, 2014). Zhou *et al.* (2014) investigated the effect of the elastic modulus of the lamina on shear strength using the planer shear test and found that the elastic modulus of the lamina did not have a statistically significant effect on CLT strength. In the planer shear test, the most significant factor affecting shear strength was the orientation of the lamina's annual rings (Li *et al.* 2021). Azin Ettelaei *et al.* (2021) evaluated shear strength of CLT made from *Eucalyptus globulus* and *Eucalyptus nitens* using a short-span bending test. A positive correlation was found between the MOE of the lamina in compression and tension and the shear strength values of the CLTs. A short-span bending test study by Navaratnam *et al.* (2020) also showed that the higher elastic modulus of Australian radiata pine lamina tends to increase the shear strength of CLT. Simon Aicher *et al.* (2016) analyzed the differences between the planer shear test and the short-span bending test. The shear strength values obtained from the planer shear test were 10% to 20% higher, and this was attributed to the fact that in the planer shear test, the compressive shear load was transferred in the major direction, resulting in pure shear failure at the outermost lamina in the major direction. This failure geometry cannot be considered as rolling shear failure, but as pure shear failure instead. Minghao Li *et al.* (2017) analyzed that in the short-span bending test, the aspect ratio of the lamina has a significant effect on the shear strength of the CLT because relatively high shear force is transmitted to the minor direction lamina due to the short span, resulting in rolling shear failure. He also mentioned that in the planer shear test, the aspect ratio of the lamina may not have a significant effect on CLT strength because relatively pure shear load is transmitted to the CLT.

This study evaluated the shear strength performance of CLT using the short span bending test method, which entails a rolling shear failure by applying a large shear load. In addition, strength was predicted by shear analysis specified by the CLT handbook and the finite element method, and the obtained values are subsequently compared with the actual value.

**MATERIALS AND METHODS**

**Fabrication of Specimens**

The lamina (t: 30 mm) used in the production of domestic *Larix kaempferi* Carr. CLT had an air-dry specific gravity of 0.58, with a standard deviation of 0.04, and an air-dry moisture content of 12.2%, with a standard deviation of 1.1%. The modulus of elasticity (MOE) of the lamina was measured by the longitudinal vibration method (Lee *et al.* 2018). The MOE of the measured lamina was mechanically graded according to KS F 3021 (Table 1). The average MOE of the graded lamina was 12.8 GPa with a standard deviation of 0.9 GPa. Phenol-resorcinol formaldehyde (PRF) resin was used to produce the CLT. The amount of adhesive applied was 400 g/m<sup>2</sup> (one-sided application) and a pressure of 1.0 MPa was likewise applied (Song and Hong 2016).

**Table 1.** Based on the Elastic Modulus of Each Grade of Lamina (KS F 3021; 2018).

Rate	E6	E7	E8	E9	E10	E11	E12	E13	E14	E15	E16	E17
Min.												
MOE (GPa)	6	7	8	9	10	11	12	13	14	15	16	17

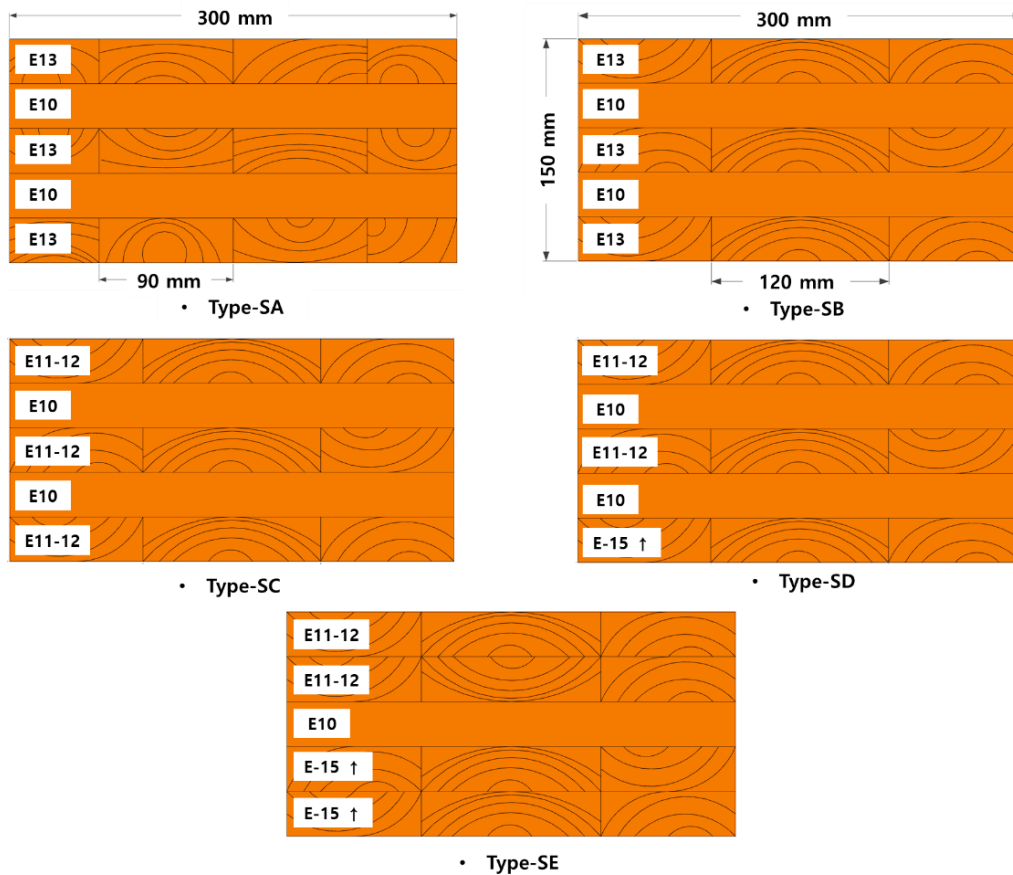


**Fig. 1.** Type of *Larix kaempferi* Carr. CLT shear specimens

Type-SA is made of 90 mm wide lamina, the MOE of the major direction lamina is E13 and the MOE of the minor direction lamina is E10 according to the C-E12-E10 standard of KS F 2081 (Fig. 1). Type-SB is made of lamina with a width of 120 mm, and MOE of the lamina was arranged as in Type-SA to compare only the effect of the width of the lamina. Unlike Type-SB, the MOE of the major direction lamina was randomized within E10 to E12 in Type-SC to investigate whether the MOE of the lamina affects the strength of CLT. In the case of Type-SD, the width of the lamina was 120 mm, the MOE of the compression lamina and the middle lamina in the major direction was same as Type-SC, and the MOE of the outermost tensile lamina was arranged as a lamina with an E15 or higher. This is because the strength of CLT is most affected by the outermost tensile lamina of CLT (Baek *et al.*, 2023). Type-SE was placed as a major direction lamina in the outermost lamina and outer lamina as shown in Fig. 1. The elastic modulus of the two laminas in the tensile part was E15 or higher, and the MOE of the two laminas in the compression part was randomly placed within E10 to E12. CLTs were made of 5 plies that were 975 mm long, 300 mm wide, and 150 mm high. Five pieces were fabricated per type.

### Shear Strength Test Method

The shear strength test was performed with short-span and three-point bending test as shown in Fig. 2. The span(l)-depth(h) ratio was 5.5:1 and the test speed was 7 mm/min (ASTM D198, 2014).

To measure the mid-span deflection of the specimen, a displacer with 50 mm maximum capacity was installed at the load point on both sides of the specimen(mid-span), and the deformation was used as the average value. The shear strength of CLT  $\tau$  CLT were calculated according to Eqs. 1.

$$\tau = \frac{3V}{2A} \quad (1)$$

$$V = \frac{P_{max}}{2} \quad (2)$$

In Eqs. 1 and 2,  $\tau$  is the maximum shear strength (MPa),  $P_{max}$  is the maximum load (N), and  $A$  is the cross-section ( $mm^2$ ),

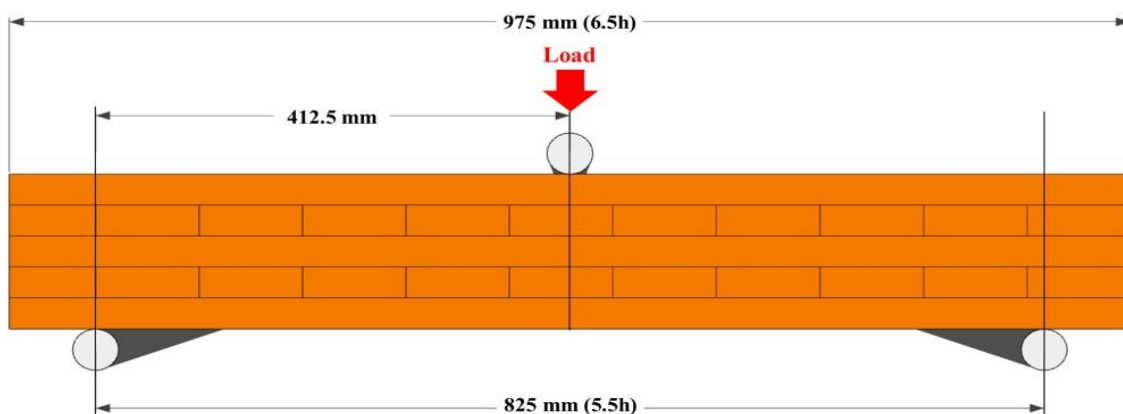


Fig. 2. Shear test setup of CLT specimens

## RESULTS AND DISCUSSION

### Short span Bending Test Result

#### *Load-deformation curve*

For Type-SA with a lamina width of 90 mm, all specimens showed elastic behavior, then localized shear failure occurred in the minor direction laminas, and then the load continued to increase until the final load (Fig. 3).

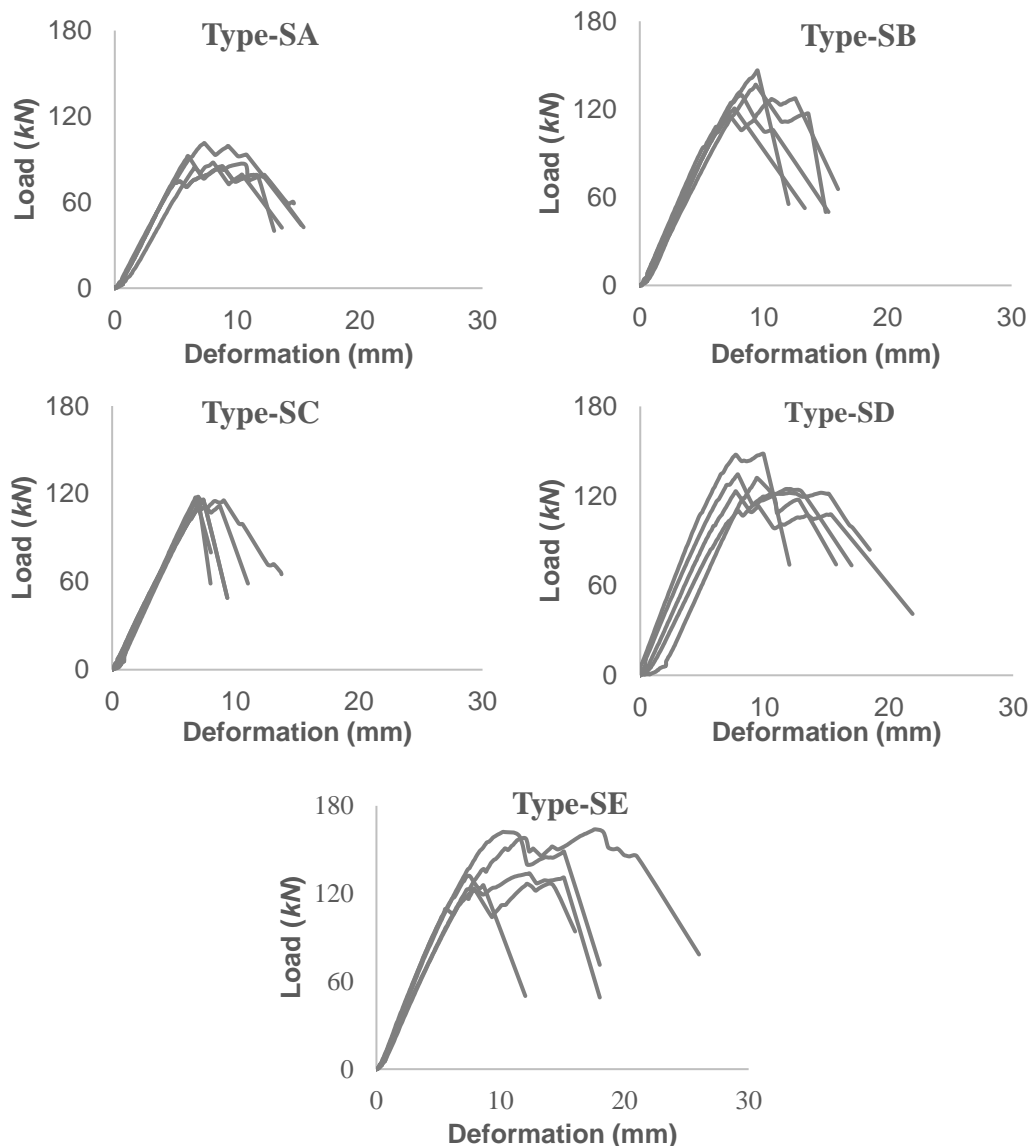


**Fig. 3.** Load and deformation curve of shear test specimens.

This load deformation behavior was also seen in shear tests of other tree species of CLT, and it seems to be a typical behavior that can be seen in short-span bending tests (Li *et al.* 2022). At the initial low load, the maximum load was the lowest among all types with an average of 89 kN due to localized failure (Table 2). However, Type-SB with a lamina width of 120 mm showed an elastic behavior up to an average maximum load of 128 kN,

and the load tended to decrease after localized failure. Two specimens showed a slight yield behavior up to the ultimate load followed by brittle failure. The remaining three specimens did not exhibit brittle failure after multiple localized fractures. For Type-SC with random elastic modulus, all specimens showed elastic behavior up to a maximum load of 119 kN without local failure, and then they showed a tendency to decrease in load after local failure.

**Table 2.** Max Load and Deformation of Specimens

Specimens		$P_{Max}$ (kN)	Ave. (kN)	Deformation (mm)	Ave. (mm)
Type-SA	1	85.1	89.5 (4.7)*	7.8	6.8 (0.7)
	2	87.7		6.0	
	3	92.3		6.1	
	4	97.3		7.3	
	5	85.1		6.8	
Type-SB	1	136.8	128.7 (4.3)	9.4	8.5 (0.7)
	2	129.6		8.3	
	3	126.4		9.5	
	4	125.2		7.8	
	5	125.5		7.8	
Type-SC	1	118.5	119.4 (3.9)	8.3	7.7 (0.5)
	2	115.5		8.1	
	3	118.0		7.0	
	4	126.9		8.0	
	5	118.3		7.3	
Type-SD	1	133.4	136.2 (9.0)	9.5	8.7 (0.9)
	2	123.2		7.7	
	3	148.1		9.9	
	4	144.5		7.8	
	5	132.1		8.5	
Type-SE	1	136.7	149.8 (11.1)	10.2	10.4 (1.1)
	2	143.8		11.4	
	3	162.2		10.2	
	4	142.4		8.6	
	5	164.0		11.6	

\*: Standard deviation

All but one specimen exhibited yield behavior up to the maximum load followed by brittle failure. The load-deformation behavior of the Type-SD specimens showed elastic behavior followed by multiple localized failures. The average maximum load was 136 kN. The deviation of each specimen from the initial load-deflection line was large, which was due to the difference between the elastic modulus of the compression lamina and the middle lamina and the elastic modulus of the outermost tensile lamina above E15. The average maximum load of Type-SE with a high elastic modulus in the outermost tensile lamina was 150 kN, the highest among all types. The three specimens failed at the knots in the outermost tensile lamina of the CLT early in the load-deformation section, showing relatively low load capacity loss. The specimens with initial localized failure had a



maximum load of 140 kN, while the specimens that showed elastic behavior with no remaining localized failure had a maximum load of 163 kN. Type-SE also exhibited a difference in the elastic modulus of the compression lamina and the middle lamina, while the outermost tensile lamina had an elastic modulus of more than E15. However, it appears that the placement of two major direction laminas in the tensile section controlled the initial load-deformation slope deviation.

#### Failure mode

When CLTs are subjected to a bending load, they typically fail at the outermost tensile section (Sikora *et al.* 2016) or undergo rolling shear failure (Song and Hong 2018). In particular, if there is a defect such as an indentation in the outermost tensile part of the CLT, the load is increased again after the first failure at the defect, and rolling shear failure subsequently occurs at the maximum load (Baek *et al.* 2021).

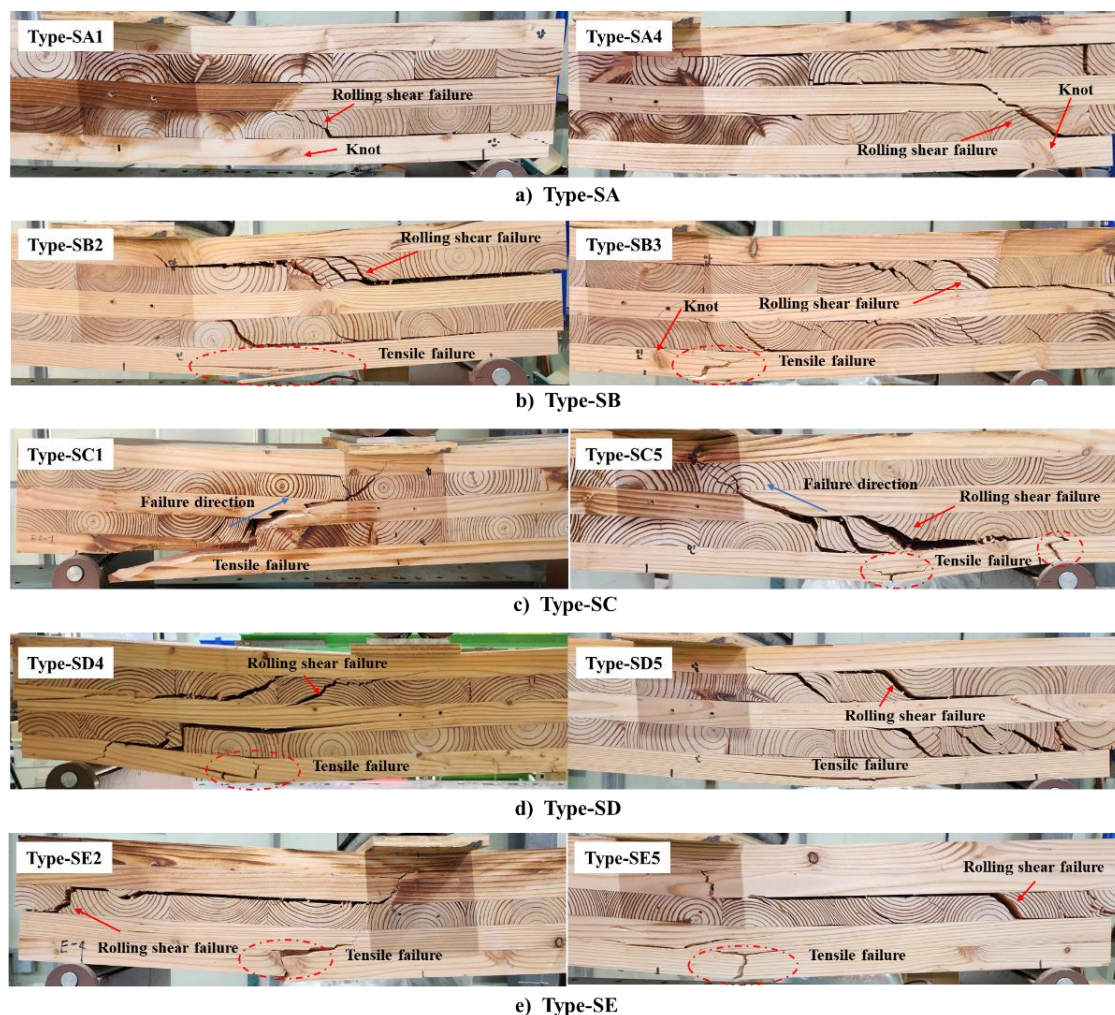


**Fig. 4.** Typical failure mode of specimens(a, b, c, d, e: Type-SA,SB, SC, SD, SE)

The failure behavior of Type-SA with a lamina width of 90 mm showed localized rolling shear failure in the minor direction lamina, followed by progression of failure in the cross-sectional direction, and finally rolling shear failure in the major direction lamina of the cross-section. Type-SA showed only rolling shear failure without tensile failure (Fig.

4a). This was similar to the failure mode of other species of CLT, and it seems to be a failure mode that appears as the span-to-depth ratio becomes smaller (Hematabadi *et al.* 2020). Furthermore, as shown in Fig. 4a, there was a knot in the outermost tensile part, but it was not destroyed, indicating that the strength of rolling shear was somewhat weaker than the failure strength in the knot. However, the Type-SB with a lamina width of 120 mm became tensile failure at the outermost tensile lamina of the CLT (Fig. 4b). This suggests that Type-SB with a lamina width of 120 mm is relatively more resistant to shear than Type-SA with a lamina width of 90 mm. After the primary failure of the outermost tensile part, rolling shear failure finally occurred. Type-SC was failure due to bearing strength and shear at the outermost tension part of the support point, and the damage progressed to the compression part (Fig. 4c). Unlike Type-SB, this failure mode did not cause cracks in the cross section, and this failure mode appears to result in brittle behavior in the load-deformation behavior. It appears that the laminas, which have a relatively low modulus of elasticity, did not carry enough load capacity. The failure mode of Type-SD exhibited primary failure at the outermost tensile part like Type-SB, followed by rolling shear failure at the annual rings of the minor direction lamina, and finally shear failure along the cross-section (Fig. 4d). Unlike the other types, when a defect such as a knot was present at the outermost tensile part of Type-SE, localized failure occurred at the knot (Fig. 4e), which contributed to the low ultimate load (Fig. 3). All specimens without defects resulted in tensile failure at the ultimate load and followed finally by rolling shear failure.

#### *Shear performance of CLT*

For the rolling shear strengths of other tree species confirmed under the same conditions of span-to-depth ratio, Irish Sitka spruce (specific gravity 0.44) CLT ranged from 1 to 2 MPa (Sikora *et al.* 2016) and Australian radiata pine (specific gravity 0.48) CLT ranged from 1.55 to 2.18 MPa (Navaratnam *et al.* 2020). The shear strength value of *Larix kaempferi* CLT was relatively high compared to other tree species, and this appears to be due to the relatively large proportion and high strength of *Larix kaempferi* (0.58) (Kim *et al.* 2021). This appears to be because the strength tends to increase relatively as the specific gravity of wood increases. The  $\tau$  for Type-SB with a lamina width of 120 mm showed a 52% improvement over Type-SA with a lamina width of 90 mm. This suggests that, unlike Type-SA, where the width of the lamina is relatively small, the load-bearing capacity of the relatively large minor direction lamina is increased, resulting in a larger shear strength value. The deviation of strength was also the lowest (Table 2), making it the most reliable in design applications. A study by Li, X (2021), in which a planer shear test was conducted with a small specimen, also showed that strength increased significantly as the width of the lamina increased. Type-SC had 10% lower  $\tau$  than Type-SB. For Type-SD  $\tau$  were 15% higher than Type-SC. It was found that simply placing a lamina with a higher elastic modulus in the outermost tensile lamina increased strength and the elastic modulus. In addition,  $\tau$  values were 6% higher than Type-SB. However, due to the difference in the elastic modulus between lamina in major directions, the variation in strength was also high. In the case of Type-E, the  $\tau$  increased by 76% compared to Type A. However, since only one lamina was placed in the minor direction to withstand rolling shear, the strength was the highest compared to other types, but the variation in strength was also the largest. Accordingly, it appears that the bending load in the major direction can be sufficiently withstood, but the bending load in the minor direction appears to have a relatively low load capacity.



**Table 3.** Experimentally derived shear properties of CLT Specimens

Specimens		Density (Kg/m <sup>3</sup> )	M.C (%)	$\tau_{max}$ (MPa)	Ave. (MPa)	Failure Mode
Type-SA	1	581	11.4	2.8	3.0 (0.22)*	Rolling shear failure
	2	601	11.7	2.9		
	3	579	11.5	3.1		
	4	580	10.2	3.4		
	5	565	11	2.8		
Type-SB	1	588	12.5	4.6	4.3 (0.13)	Tensile failure and Rolling shear failure
	2	540	11.7	4.3		
	3	568	13.5	4.2		
	4	598	12.2	4.2		
	5	617	11.5	4.2		
Type-SC	1	553	11.6	4.0	4.0 (0.15)	Tensile failure and Rolling shear failure
	2	584	12.4	3.8		
	3	513	11.6	3.9		
	4	557	10.5	4.2		
	5	580	10.9	3.9		
Type-SD	1	592	11.6	4.4	4.5 (0.29)	Tensile failure and Rolling shear failure
	2	565	11.6	4.1		
	3	626	10.9	4.9		
	4	555	11.7	4.8		
	5	629	12.1	4.4		
Type-SE	1	580	11.2	4.6	5.0 (0.37)	Tensile failure and Rolling shear failure
	2	620	11.3	4.8		
	3	612	11.7	5.4		
	4	630	12.3	4.7		
	5	593	12.4	5.5		

\*: standard deviation

### Shear Strength Prediction through Theoretical Analysis

#### *Simplified method*

In the CLT Handbook it is stated that the simplified method can be used for design of bending members resisting load perpendicular to the plane of the CLT. The simplified method for bending strength has also been adopted in the product standard PRG 320. Similar to the bending strength, a simplified method using the extreme fiber capacity of shear is also available and has been proposed for the PRG 320 product standard. Using the simplified method, an effective shear load,  $V_{eff}$  can be calculated as Eq. 3. The effective bending stiffness  $(EI)_{eff}$  of CLT was calculated using Eq. 4. Since CLT is laminated orthogonally to the fiber direction of the lamina, the shear strength ( $f_v$ ) of longitudinal (fiber) direction-tangential or radial direction for larch lamina was applied 3.3 MPa (Baek *et al.* 2023),

$$V_{eff} = f_v(lb/Q)_{eff} \quad (3)$$

$$(Ib/Q)_{eff} = \frac{EI_{eff}}{\sum_{i=1}^{n/2} E_i h_i a_i} \quad (4)$$

$$EI_{eff} = \sum_{i=1}^n (E_i I_i + E_i A_i a_i^2) \quad (5)$$

$$a_2 = \frac{E_1 A_1 (\frac{h_1}{2} + \frac{h_2}{2}) - E_3 A_3 (\frac{h_2}{2} + \frac{h_3}{2})}{\sum_{i=1}^3 E_i A_i} \quad (6)$$

where  $V_{eff}$  = induced shear due to loads (N),  $f_v$  = shear strength of *Larix kaempferi* (MPa),  $I$  = moment of inertia of CLT ( $mm^4$ ),  $b$  = width of the cross-section of CLT (mm),  $Q$  = static moment of area for the cross-section ( $mm^3$ ),  $EI_{eff}$  = Effective bending stiffness of CLT ( $mm^2$ ),  $E_i$  = MOE of lamina (N/mm<sup>2</sup>),  $h_i$  = depth of lamina (mm),  $a_i$  = distance between the center of a lamination to the neutral axis (mm),  $I_i$  = Geometry moment of lamina ( $mm^4$ ), and  $A_i$  = Cross section ( $mm^2$ ),

The load capacity ( $V_{eff}$ ) predicted by the simplified method is shown in Fig 5. Type-A and Type-B have the same predicted  $V_{eff}$ , which is due to the same MOE of the lamina used, and also because the width of the lamina is not considered. For Type-SA with a layer width of 90 mm, the prediction error was the highest at 41%. However, for Type-SA with a lamina width of 120 mm, the prediction error was 2%, which is close to the measured value. Therefore, it seems that the load-bearing capacity of CLT is low for Type-SA with 90 mm layer width because the layer does not have enough shear resistance, while for Type-SA with 120 mm layer width, the layer is large enough to withstand the shear application. Type-SC is underestimated by about 7% because the MOE of the lamina comprising Type-SC (12.3 GPa) is relatively low compared to the MOE of the lamina comprising Type-SB (14.5 GPa). The prediction error rate of Type-SD and Type-SE was 2%, which is similar to the actual value, confirming that the MOE of the outermost tensile has an influence on the shear strength of CLT.

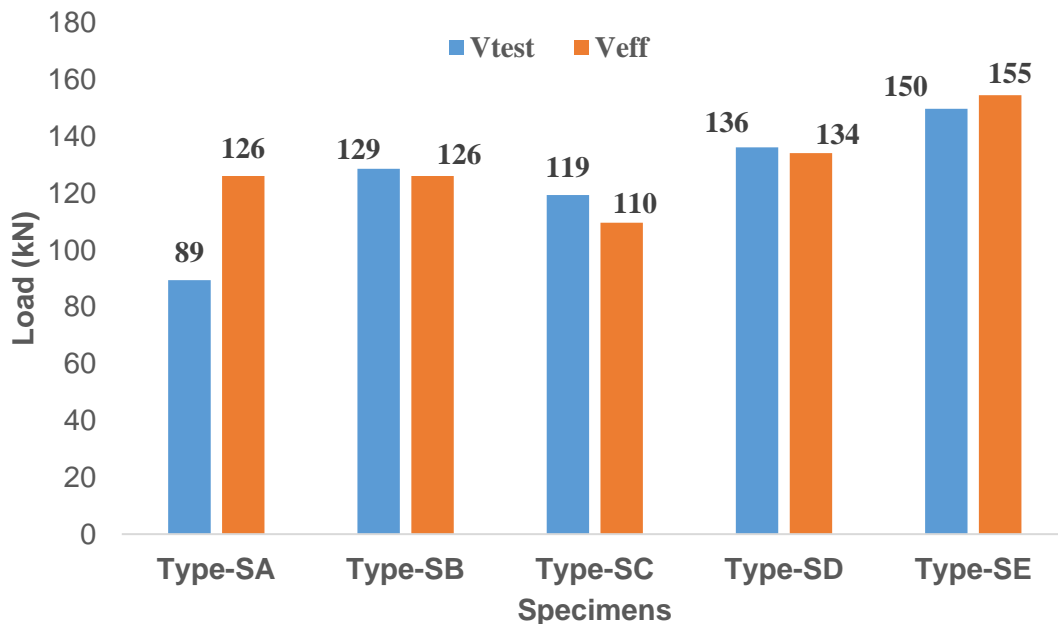


Fig. 5. Comparing predicted  $V$  ( $V_{eff}$ ) and Experiment result  $V$  ( $V_{test}$ )

## Shear Strength Analysis through FEM Model

### *Finite element analysis by FEM modeling*

The finite element analysis was performed using the ANSYS program (ANSYS 17.0). The material constants for each CLT type were taken from Table 4. The MOE of the lamina used in CLT production was applied as  $E_L$ , for the remaining material constants, values from Baek *et al.* (2023) were used based on the MOE ( $E_L$ ),  $E_R$  was applied to  $E_L/12$ ,  $E_T$  to  $E_L/14$ ,  $G_{LR}$  to  $E_L/18$ ,  $G_{RT}$  to  $E_L/123$ , and  $G_{LT}$  to  $E_L/22$ .

**Table 4.** Material Model Inputs for the Finite Element Analysis

Material constant	Density (kg/m <sup>3</sup> )	$E_L$ (MPa)	$E_R$ (MPa)	$E_T$ (MPa)	$\nu_{LR}$	$\nu_{RT}$	$\nu_{LT}$	$G_{LR}$ (MPa)	$G_{RT}$ (MPa)	$G_{LT}$ (MPa)
E10	560	10000	813	674	0.357	0.606	0.493	558	81	451
E11	560	11000	1008	837	0.357	0.606	0.493	692	100	560
E13	560	13000	1170	970	0.357	0.606	0.493	800	110	650
E15	560	15000	1375	1140	0.357	0.606	0.493	945	137	765

L: Longitudinal direction, R: Radial direction, T: Tangential direction

The finite element analysis was modeled identically to the actual test. The finite element model was a 3D model, a cube, and the element size was set to 15 mm. There were 8640 elements and 19749 nodes. The size of the support point was the same as the size of the point used in the actual test. The support was set to be fixed. The boundary condition between the support and the specimen was set to frictional, which allows the point to slide, since it is a rollover point, while the friction coefficient was set to 0.5. The large deflection option was set switched on because the bending strength test causes large deformation values. The inter-lamina adhesion condition was set to bonded. The initial substep was defined as 100 and the maximum substep as 5000. The loading target of the specimen was set as the loading point as in the actual test, and the direction was a unidirectional line pointing downward from the loading point. The load was set as a deformation, and all specimens were subjected to the same deformation of 8 mm. Shear Stress was selected in the analysis area to review the shear stress acting on the cross-section of each specimen.

The load-deformation behavior by FEM for each type is shown in Fig. 7. The shear stress analysis using the finite element method showed that Type-SA, SB, SC, and SD had the largest shear strength between the outermost tensile lamina and the fiber orthogonal lamina in the tensile zone (Fig. 6). Type-SA was 2.5 MPa, Type-SB was 4.5 MPa, Type-SC was 3.5 MPa, Type-SD was 4.4 MPa, and Type-SE was 5.0 MPa. Type-SA and Type-SB yielded results different from that predicted by the CLT Handbook's simplified method analogy because the finite element analysis took into account the lamina's width. The stress distribution obtained from the finite element analysis was found to be relatively closer to the measured values than the theoretical analysis. Figure 6 showed the largest distribution of shear stresses between the outermost major and minor direction laminas. This is believed to be due to the relatively weak shear strength between the outermost major and minor directional laminas because the laminas are orthogonally stacked to each other (Baek *et al.* 2023). Type-SE showed that the shear stress between the major direction lamina and the center minor direction lamina was the largest, rather than the shear stress between the outermost tensile major direction lamina and the adjacent major direction lamina.

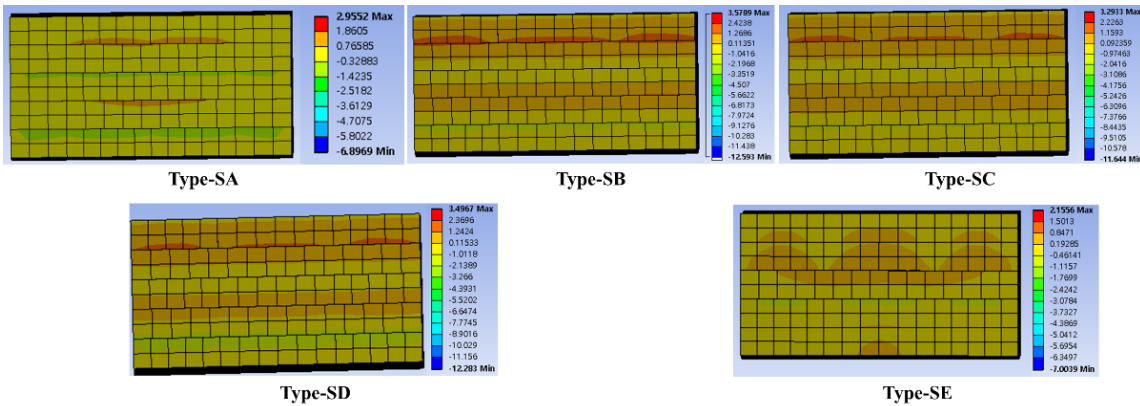


Fig. 6. Results of shear stress distribution analysis in cross section

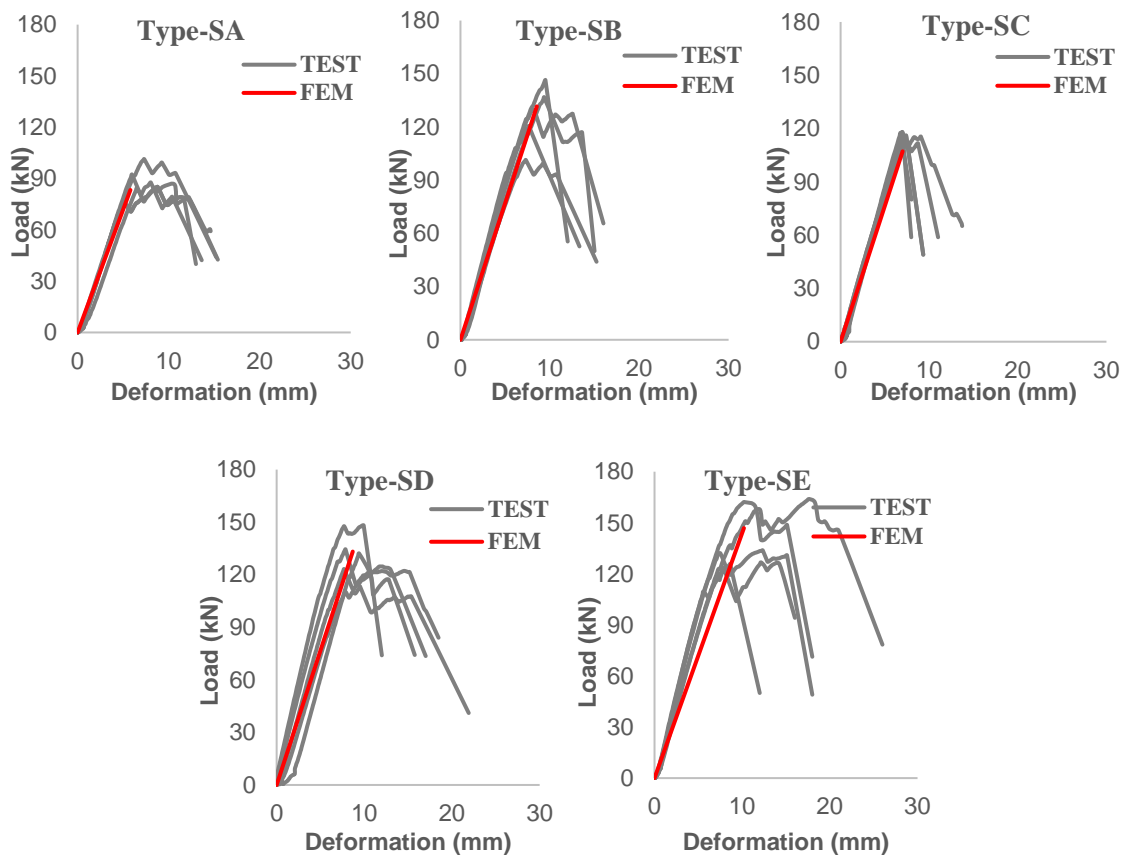


Fig. 7. Load-deformation curve by Test result and FEM analysis of each type.

## CONCLUSIONS

1. When the elastic modulus of the lamina comprising the cross-laminated timber (CLT) was the same, the domestic *Larix kaempferi* Carr. CLT with relatively small lamina widths had low shear strength due to rolling shear failure. CLTs with relatively large lamina widths underwent rolling shear failure and failure of the outermost tensile lamina, which resulted in relatively higher shear strength and lower deviation than CLTs with smaller lamina widths.

2. The shear strength of the CLT was also affected by the modulus of elasticity (MOE) of the outermost tensile lamina, as the relatively higher placed MOE of the outermost tensile lamina controlled the bending stresses and thus subjected it to higher loads.
3. For domestic *Larix kaempferi* Carr. CLT with 90 mm wide laminas, the predicted value in the shear analogy was 41% higher than the measured value. However, the prediction error rate through theoretical analysis for the 120 mm wide specimen was 2%, which indicated that the 120 mm wide lamina had sufficient ability to withstand the applied shear according to the design. The shear strength prediction through theoretical analysis of CLT based on the MOE of the lamina was also similar to the actual value.
4. The shear stress from the finite element analysis was different from theoretical analysis because the width of the lamina was considered. The shear stress distribution in the cross-section from the finite element analysis showed that the largest shear stresses occurred between the outermost tensile major direction lamina and the minor direction lamina. This is because the fiber orientations of the laminas are orthogonal to each other, resulting in low capacity to resist applied shear stresses.

## ACKNOWLEDGEMENTS

This work was supported by the National Research Foundation of Korea (NRF) grant funded by the Korea government (MSIT) (No. 2022R111A3072085).

## REFERENCES CITED

- Aicher, S., Hirsch, M., and Christian, Z. (2016). "Hybrid cross-laminated timber plates with beech wood cross-laminas," *Construction and Building Materials* 124, 1007-1018. DOI: 10.1016/j.conbuildmat.2016.08.051
- ASTM D198 (2014). "Standard test methods of static tests of lumber in structural sizes," American Society for Testing and Materials, West Conshohocken, PA, USA.
- Baek, S. Y., Song, Y. J., Kim, H. W., and Hong, S. I. (2023). "Bending strength prediction and finite element analysis of larch structural beams," *BioResources* 18(1), 1824-1835. DOI: 10.15376/biores.18.1.1824-1835
- Baek, S. Y., Song, Y. J., Yu, S. H., Kim, D. H., and Hong, S. I. (2021). "Bending performance of cross-laminated timber-concrete composite slabs according to the composite method," *BioResources* 16(4), 8227-8238 DOI: 10.15376/biores.16.4.8227-8238
- CSA 086: 19 (2019). *Engineering Design in Wood*, Canadian Standards Association, Mississauga, CSA
- Chong, S., Won, K., Hong, N., Park, B., Lee, K., and Byeon, H. (2014). "Bending and compressive strength properties of *Larix kaempferi* according to thinning intensity," *Journal of the Korean Wood Science and Technology* 42(4), 385-392. DOI: 10.5658/wood.2014.42.4.385
- Ehrhart, T., and Brandner, R. (2018). "Rolling shear: Test configurations and properties of some European soft-and hardwood species," *Engineering Structures* 172, 554-572. DOI: 10.1016/j.engstruct.2018.05.118
- Ettelaie, A., Taoum, A., and Nolan, G. (2021). "Rolling shear properties of cross-



- laminated timber made of fibre-managed plantation eucalyptus under short-span bending,” *Wood Material Science & Engineering* 17(6), 744-751. DOI: 10.1080/17480272.2021.1942201
- EN 16351 (2015). “Timber structures –Cross laminated timber,” European Committee for Standardization, Belgium, Germany
- Gagnon, S., and Pirvu, C. (2011). “CLT Handbook: Cross-laminated Timber,” FPIInnovations, Quebec City, Canada.
- Hematabadi, H., Madhoushi, M., Khazaeyan, A., Ebrahimi, G., Hindman, D., and Loferski, J. (2020). “Bending and shear properties of cross-laminated timber panels made of poplar (*Populus alba*),” *Construction and Building Materials* 265, article 120326. DOI: 10.1016/j.conbuildmat.2020.120326
- Kim, S. H., Kim, D. H., Jo, J. I., Kim, J. H., Lee, S. H., Choi, J. K., and Kim, N. H. (2021). “A comparative study on the physical and mechanical properties of Dahurian larch and Japanese larch grown in Korea,” *Wood Research* 66(2), 415-426. DOI: 10.3390/f13071074
- KS F 2081 (2021). “Cross laminated timber,” Korean Standards Association, Seoul, Korea.
- Kwon, K., Han, H., Seol, A., Chung, H., and Chung, J. (2013). “Development of a wood recovery estimation model for the tree conversion processes of *Larix kaempferi*,” *Journal of Korean Society of Forest Science* 102(4), 484-490. DOI: 10.14578/jkfs.2013.102.4.484
- Lee, I. H., Cho, S. M., and Hong, S. I. (2018). “Prediction of the MOR of larch lumber,” *Journal of the Korean Wood Science and Technology* 46(1), 93-99. DOI: 10.5658/wood.2018.46.1.93
- Li, H., Wang, L., Wei, Y., Wang, B. J., and Jin, H. (2022). “Bending and shear performance of cross-laminated timber and glued-laminated timber beams: A comparative investigation,” *Journal of Building Engineering* 45, article 103477. DOI: 10.1016/j.job.2021.103477
- Li, M. (2017). “Evaluating rolling shear strength properties of cross-laminated timber by short-span bending tests and modified planar shear tests,” *Journal of Wood Science* 63(4), 331-337. DOI: 10.1007/s10086-017-1631-6
- Li, X., Ashraf, M., Subhani, M., Kremer, P., and Li, H., and Anwar-Us-Saadat, M. (2021). “Rolling shear properties of cross-laminated timber (CLT) made from Australian Radiata Pine—An experimental study,” *Structures* 33, 423-432. DOI: 10.1016/j.istruc.2021.04.067
- Navaratnam, S., Christopher, P. B., Ngo, T., and Le, T. V. (2020). “Bending and shear performance of Australian Radiata pine cross-laminated timber,” *Construction and Building Materials* 232, article 117215. DOI: 10.1016/j.conbuildmat.2019.117215
- Rahman, M. D., Ashraf, M., Ghabraie, K., and Subhani, M. (2020). “Evaluating Timoshenko method for analyzing CLT under out-of-planer loading,” *Buildings* 10(10), article 184. DOI: 10.3390/buildings10100184
- Sikora, K. S., McPolin, D. O., and Harte, A. M. (2016). “Effects of the thickness of cross-laminated timber (CLT) panels made from Irish Sitka spruce on mechanical performance in bending and shear,” *Construction and Building Materials* 116, 141-150. DOI: 10.1016/j.conbuildmat.2016.04.145
- Song, Y. J., and Hong, S. I. (2018). “Performance evaluation of the bending strength of larch cross-laminated timber,” *Wood research* 63(1), 105-116.
- Song, Y. J., and Hong, S. I. (2016). “Evaluation of bonding strength of larch cross-

laminated timber,” *Journal of the Korean Wood Science and Technology* 44(4), 607-615. DOI: 10.5658/wood.2016.44.4.607

Wang, Z., Zhou, J., Dong, W., Yao, Y., and Gong, M. (2018). “Influence of technical characteristics on the rolling shear properties of cross laminated timber by modified planar shear tests,” *Maderas Ciencia y Tecnología* 20(3), 469-478. DOI: 10.4067/s0718-221x2018005031601

Zhou, Q. Y., Gong, M., Chui, Y. H., and Mohammad, M. (2014). “Measurement of rolling shear modulus and strength of cross-laminated timber using bending and two-plate shear tests,” *Wood and Fiber Science* 46(2), 259-269. DOI: 10.1109/bmse.2012.6466175

Article submitted: February 15, 2024; Peer review completed: March 9, 2024; Revised version received and accepted: May 7, 2024; Published: May 16, 2024.  
DOI: 10.15376/biores.19.3.4366-4380